J. Am. Soc. Mass Spectrom. (2019) 30:2637–2645
DOI: 10.1007/s13361-019-02330-3

RESEARCH ARTICLE

Enhanced Multiplexing in Fourier Transform Charge Detection Mass Spectrometry by Decoupling Ion Frequency from Mass to Charge Ratio

Conner C. Harper, Evan R. Williams

Department of Chemistry, University of California, Berkeley, CA 94720-1460, USA

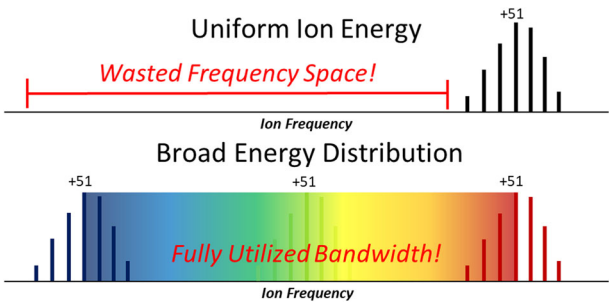

Abstract. Weighing single ions with charge detection mass spectrometry (CDMS) makes it possible to obtain the masses of molecules of essentially unlimited size even in highly heterogeneous samples, but producing a mass histogram that is representative of all of the components in a mixture requires substantial measurement time. Multiple ions can be trapped to reduce analysis time but ion signals can overlap. To determine the maximum gains in analysis speed possible with current instrumentation with multiple ion trapping, simulations calculating the frequency and overlap rate of ions with different mass, charge, and energy ranges were performed. For an analyte with a broad mass distribution, such as long chain polyethylene glycol (PEG, 8 MDa), gains in analysis speed of up to 160 times that of prior CDMS experiments are possible. For signals from homogeneous samples, ions with the same *m*/*z* have frequencies that overlap and interfere, reducing the effectiveness of multiplexing in experiments where ions have the same energy per charge. We show that by maximizing the decoupling of ion *m*/*z* from frequency using a broad range of ion energies, the rate of signal overlap is significantly reduced making it possible to trap more ions. Under optimum decoupling conditions, a measurement speed nearly 50 times greater than that of prior CDMS experiments is possible for RuBisCO (517 kDa). The reduction in overlap due to decoupling also results in more accurate quantitation in samples that contain multiple analytes with different concentrations.

Keywords: CDMS, Charge detection mass spectrometry, Multiplexing, Fourier transform, Megadalton, Ion energy, Ion frequency, High-throughput, Decoupling, Native MS

Received: 3 June 2019/Revised: 27 August 2019/Accepted: 28 August 2019 /Published Online: 12 November 2019

Introduction

Native mass spectrometry, in which ions of biomolecular molecules and associated macromolecular complexes are produced by electrospray ionization from aqueous solutions containing 100+ mM concentrations of salts [1, 2], is widely used to obtain structural information about molecular ions formed from environments in which they have native structures and reactivities [3]. Information about the stoichiometries and structures of complexes can be obtained from tandem mass spectrometry experiments in which mass-selected precursor ions are activated, either through collisions with gaseous molecules or with surfaces, and the resulting fragment ions, typically consisting of intact monomer subunits or sub-assemblies, are mass analyzed [4, 5]. A key challenge in extending the mass range of analytes amendable to such measurements is the need to resolve individual charge states in order to obtain molecular weight information from larger species, such as intact viruses [6]. This is particularly challenging for complex samples, such as synthetic polymers [7, 8] or intrinsically heterogeneous macromolecular complexes, where charge-state distributions of the individual components in the mixture are unresolved [9]. Signals for each component in an ensemble measurement can overlap and can lead to loss of resolved signal. In these

Electronic supplementary material The online version of this article (https://doi.org/10.1007/s13361-019-02330-3) contains supplementary material, which is available to authorized users.

Correspondence to: Evan Williams; *e-mail:* erw@berkeley.edu

cases, tandem mass spectrometry performed on a narrow range of *m/z* precursors can spread out the fragment ion signal over a wider range of *m/z* and enable some mass information to be obtained [9, 10].

One method to overcome the problem of heterogeneity is to mass analyze individual ions so that the measurement of one ion does not interfere with the measurement of another. Single-molecule mass measurements have been demonstrated using a variety of different methods, including nanoelectromechanical systems [11, 12] and with various types of mass spectrometers, including Fourier-transform ion cyclotron resonance (FTICR) [13, 14], Orbitrap [15, 16], ion trap [17–21], cryodetector time-of-flight [22, 23], and charge detection mass spectrometry (CDMS) [24–30]. Several of these mass spectrometry methods can provide high mass measuring accuracy but this typically comes at the expense of analysis time. Kafader et al. demonstrated a resolving power of 677,000 from single-ion measurements in an Orbitrap mass spectrometer for the protein carbonic anhydrase using ~ 250 ms measurement times, but found that there was significant ion decay for species over 40 kDa which resulted in "hours of total acquisition time to produce a composite mass spectrum with statistically meaningful isotopic distributions" [16].

In order to obtain useful information about the composition of heterogeneous samples, the masses of many individual ions must be measured [26]. Thus, analysis speed is essential for practical single-ion measurements. Single-ion Fourier transform charge detection mass spectrometry (FT-CDMS), in which individual ions are confined in an electrostatic ion trap and the *m/z* of each ion is obtained from its oscillation frequency, can provide useful mass measurements from molecules of essentially unlimited size, ranging from small proteins up to particles with masses well above 100 MDa [26, 27, 31–39]. Detection and mass accuracy depend on a number of factors, including the ion charge and trap time, but useful measurements can be made in about 100 ms [31, 32, 34, 40], although longer trapping times are often used to improve mass measurements [41] or to obtain single-ion collisional cross sections [38, 39] or MS^n information [37] in combination with the measurements of individual ion masses. Because large macromolecules and macromolecular complexes typically have a large number of non-volatile salts and often solvent molecules attached, the masses of large complexes that can be measured in conventional mass spectrometers are often higher than those of the computed masses. Robinson and co-workers have reported a widely used method, which relates the peak width of a charge state to the extent of adduction to provide a "corrected" mass of the unadducted complex [9]. The mass attributed to adduction can account for more than ~ 1% of the overall measured mass for large protein assemblies weighing 385–800 kDa [9]. The extent to which large molecules and complexes are adducted limits the overall need for high mass measuring accuracy because the ultimate mass accuracy is limited by any correction method for larger ions [6, 9]. Thus, a mass accuracy of less than 0.1%, readily achievable in CDMS with 100 ms trap times and samples of 1000+ ions [26, 42, 43], should not limit the overall mass accuracy with which large complexes, polymers, or viruses can be weighed.

Even with a 100 ms trap time, the number of ions that can be measured per second is limited by weighing just one ion at a time. Until recently, it was believed that single-ion trapping events were required in FT-CDMS. Jarrold and co-workers state: "…multiple ion trapping events cannot be analyzed because two highly charged ions trapped together interact and perturb the oscillation frequencies. Hence, only single ion trapping events are useful" [26]. In order to achieve the optimum single-ion trapping conditions, the ion current has to be carefully regulated so that a single ion is trapped in only 37% of the measurements [26, 44]. Lower currents lead to fewer single-ion trapping events and higher currents lead to more trapping of multiple ions at the expense of single-ion events. Thus, under optimum single-ion conditions, fewer than four ions can be weighed per second using 100 ms trap times and nearly 2/3 of the measurements, which contain no or multiple ions, are discarded [26, 44].

We recently demonstrated that multiple trapped ions can be individually weighed in FT-CDMS and that ion-ion interactions with up to 21 ions trapped do not affect the mass measuring accuracy or ion trapping for times up to 1 s [43]. A key issue, however, is when two or more ions of the same or similar *m/z* are introduced into the trap and the resulting signals overlap in frequency. This greatly complicates individual ion mass measurement and is most likely for homogenous samples where the number of charge states in a charge-state distribution is limited. This problem of ion overlap can be significantly reduced by decoupling the ion frequency from the ion *m/z* [43]. This decoupling is accomplished by introducing a relatively broad distribution of ion energies per charge (hereafter referred to simply as "ion energies" or "energies") into the ion trap and measuring the energy of each ion in situ. A greater than 10-fold gain in speed was demonstrated with multiple single-ion measurements using this frequency to *m/z* decoupling scheme [43]. Here, we explore the limits of multiple ion trapping experiments and how various instrument and analysis parameters affect the potential signal increases in these measurements. These results indicate that this scheme should make possible rapid acquisition of masses of constituent molecules and that this method will be particularly useful for samples that are not amenable to analysis using conventional mass spectrometry measurements.

Theory

Decoupling Ion Frequency and m/z in CDMS

In conventional mass spectrometry, a single observable is directly coupled to the *m/z* of an analyte ion. For example, in the most widely used high-performance Fourier-transform mass spectrometry instruments, such as Fourier-transform ion cyclotron resonance (FTICR) or Orbitrap instruments, ion *m/z* is generally determined by calibrating the measured ion frequencies to a *m/z* scale using reference standards with known

mass [45]. While other factors, such as magnetic field strength (FTICR), injection distance from the axial minimum potential (Orbitrap), and trap geometry (both), also affect the observed ion frequencies, they are held constant with a high degree of precision, leaving ion m/z as the sole variable which makes possible direct calibration of ion frequency to ion m/z. In FT-CDMS, where ions are trapped and oscillate with a period frequency, the relationship between ion frequency, f, and m/z, given in Eq. (1):

$$\frac{m}{z} = \frac{C(E)}{f^2} \tag{1}$$

$C(E)$ is a function of ion energy, the trapping voltage, and the trap geometry. This value is determined from ion trajectory simulations [38, 39]. Thus, the ion frequency depends on ion energy, through $C(E)$, as well as ion m/z. In most FT-CDMS trapping experiments to date, $C(E)$ is kept constant with a narrow bandwidth of energies selected by using energy selective ion optics, such as a dual hemispherical deflection analyzer [46] or a turning quadrupole [29]. The narrowest spread of ion energies reported in single-ion CDMS is a standard deviation of 0.3% of the nominal energy, which makes possible the charge-state resolution of analytes as large as 465 kDa [42].

The necessity for energy selective ion optics can be eliminated if the ion energy is determined directly from individual ion signals. Because the duty cycle of the time domain ion signal in FT-CDMS depends on the ion energy, the amplitudes of the fundamental and harmonic frequencies also depend on ion energy [39]. Thus, the ratio of the fundamental and second harmonic frequencies can be used to dynamically determine the ion energy throughout the entire trapping period [39]. This measurement of ion energy does not depend on the ion frequency.

Dynamically measuring ion energies makes it possible to take advantage of the ion m/z and frequency decoupling that occurs as result of non-uniform ion energies in CDMS. Figure 1 demonstrates the advantages that can be gained by intentionally decoupling ion m/z and frequency. The m/z spectrum of RuBisCO (517 kDa) acquired using a commercial quadrupole time-of-flight mass spectrometer [43] is shown in Figure 1a. The most abundant or base peak corresponds to the + 51 charge state at $m/z \sim 10{,}140$. The theoretical frequency line spectrum of the same RuBisCO ions that would be measured in a conventional FT-based instrument or a CDMS spectrum where the ion energy is a singular value, i.e., $C(E)$ in Eq. (1) is a constant, is shown in Figure 1b. If a broad range of ion energies are introduced into the trap, the m/z and frequency are no longer directly coupled. This is illustrated in Figure 1c in which an ion with a given m/z can be observed anywhere within a range of frequencies that is determined by the width of the ion energy distribution.

The decoupling of ion frequency and m/z is important to increasing the number of ions that can be simultaneously analyzed in a single CDMS trapping event. Because FT-

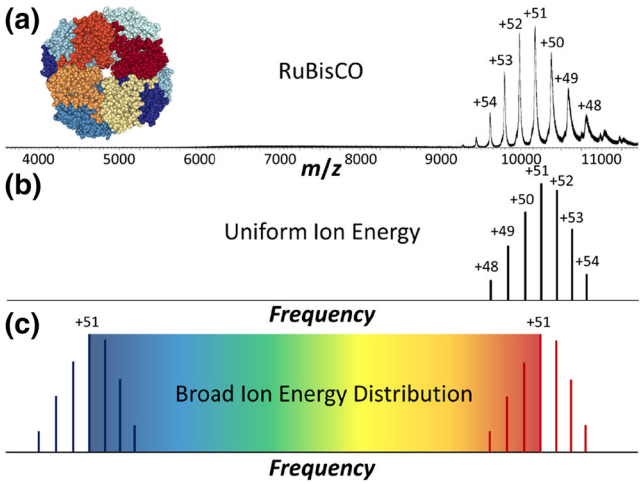

Figure 1. Illustration of decoupling ion m/z from ion frequency. The m/z spectrum of RuBisCO (517 kDa, with structure PDB ID: 8RUC shown in the left corner) obtained using a commercial Q-TOF instrument (**a**) has a limited number of peaks in the charge state distribution. An equivalent theoretical frequency domain spectrum that might be measured using a conventional FT-based instrument or a CDMS instrument where the range of ion energies is narrow is shown in (**b**). By introducing a broad range of ion energies into a CDMS instrument, m/z and frequency are decoupled. Thus, ions that have the same m/z can appear at different frequencies, as shown in (**c**). If multiple ions are trapped, the probability of ion interference in (**b**) is high, but low in (**c**)

CDMS is based on individual ion frequency and amplitude measurements, two or more ions with interfering frequencies and convolved amplitudes provide no mass information. For example, if two ions with the same m/z and energy are trapped simultaneously, analogous to a single peak in the spectrum in Figure 1b, their signals would interfere and the mass of neither ion could be readily determined. This is almost certain to occur as the number of trapped ions approaches the number of peaks in the charge-state distribution of a relatively pure sample of a large molecule, significantly limiting the possibility of multiple ion measurements in cases where mass measuring accuracy is on the order of the peak width. By maximizing the frequency range in which ions of a given m/z can be observed (Figure 1c), the probability of interferences is greatly reduced. This makes it possible to introduce and simultaneously measure a greater number of ions in a single trapping event, decreasing the time required to measure a representative mass spectrum. Detection and analysis of simultaneously trapped individual ions have been recently demonstrated in CDMS [43]. Data from ion trapping events containing multiple RuBisCO ions with a moderately broad distribution of ion energies (standard deviation of ~ 3% of nominal centroid energy) resulted in more than an order of magnitude decrease in data acquisition times over optimal measurements of just single trapped ions [43].

In other FTMS methods, including FTICR, Orbitrap, and CDMS for ensemble measurements of low charge-state ions, ion motion must be coherent in order to measure ion mass. Space-charge effects can be observed when the number of

charges of trapped ions with similar *m/z* exceed a certain value. For example, effects on FTICR frequencies have been measured when ~ 10,000 charges are present in the trap [45, 47]. This can result in signal coalescence, a loss of resolution, and other errors [45, 47]. Another advantage of single-ion CDMS is that ion motion does not have to be coherent in order to measure ion masses. In fact, for optimum multiplexed ion measurements, ion coherence is highly undesirable because coherent ions with the same or nearly the same *m/z* and frequency will experience more ion-ion interactions. Incoherent ions interact for only brief periods of time, making it possible to simultaneously trap a greater number of ions without significant space-charge effects. Decoupling ion frequency from *m/z* decreases ion coherence as ions with the same *m/z* are not constrained to a single oscillation frequency. Incoherence can be also achieved by using ion injection times that are longer than the oscillation period of the lowest velocity ions, effectively randomizing the initial phase of ion oscillation.

Methods

Simulating CDMS Ion Frequencies

In order to find the maximum possible decrease in data acquisition times using existing CDMS instrumentation [37], simulations of multiple ion trapping events were performed using a program written in Python (Supporting Information). The effects of many different variables, including the number of ions within a single trapping event, ion charge, charge-state distribution width, ion mass, ion mass distribution width, nominal ion energy, ion energy distribution width, and FT peak width, were investigated. For each number of ions within a single trapping event, hereafter referred to as the "ion count", 1000 trapping events were simulated to insure statistically meaningful results. Each ion in the simulation was assigned with mass, charge, and energy values randomly generated from Gaussian probability distributions where the mean and standard deviation for each property are given as parameters in the simulation. For ion mass and charge, parameters are chosen to match a real analog as closely as possible. Ion energy distributions are chosen to match instrumental conditions that enable different extents of frequency and *m/z* decoupling. The electrostatic cone trap used in previous CDMS experiments can stably trap a relatively broad range of ion energies (±~ 12% of trap centroid energy) [37, 39]. However, when very broad ion energy distributions are introduced to the trap, some ions fall outside of this range of stability. Initially generated ion energies outside of the stable trapping range are reevaluated until the energy generated falls within the stable range, yielding a Gaussian distribution of energies that is truncated at low and high energy.

The ion simulation process is shown schematically in Figure 2. For the charge-state distribution, the randomly generated values are rounded to the nearest integer value, shown in Figure 2 (top) as the black curve and corresponding black stick plot. The ion energies and the additional parameter of the ion trap voltage are then used to calculate the values of $C(E)$ in Eq. (1) for each ion [39], which, along with the individual ion masses and charges, are used to calculate the frequency of each simulated ion. For each charge state, the distributions of possible frequencies originating from mass (red) and energy (blue) distributions are shown in Figure 2 (top). In Figure 2, the ranges of possible frequencies due to a broad spread of ion energies cut off abruptly due to trap stability constraints, but are still much larger than those due to the narrow spread of ion masses. This result is typical of the relatively homogeneous samples that are often analyzed with native mass spectrometry. After the frequencies are calculated for ions within a single trapping event, the final step of the simulation evaluates overlap between ion frequencies. In a real CDMS trapping event, if the frequencies of two or more ions are closer than the characteristic FT peak width, they interfere with each other, making it difficult to properly measure the exact frequency and charge of the ions. Thus, in these simulations, ions in the same trapping event that have frequencies closer than the FT peak width are discarded. Figure 2 (bottom) shows an example of simulated trapping event where the ion count is 10 and two ions with overlapping frequencies near the center of the overall distribution are discarded. Such overlapping ion signals in CDMS measurements are readily identified owing to minor differences in ion frequency evolution with time [43]. Simulated ions that survive this culling criterion could be accurately measured in a real CDMS experiment. The surviving ions from all trapping events at each ion count are summed and divided by the number of trapping events to yield the average number of usable ions at each ion count. To determine the overall gain in ion throughput relative to single ion-only CDMS analysis,

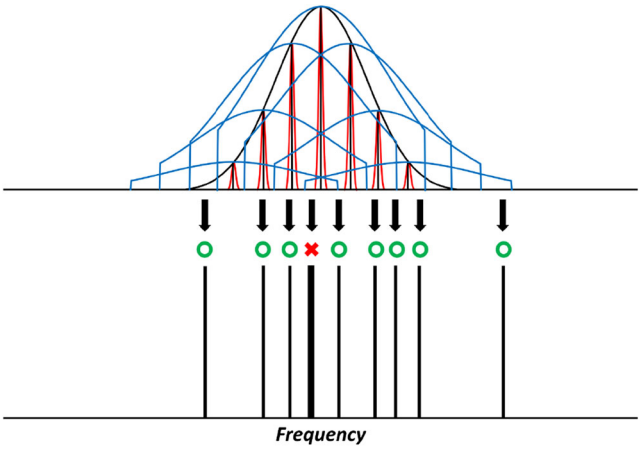

Figure 2. Scheme of the ion frequency simulation of a trapping event with an ion count of 10. Gaussian-weighted, randomly generated values for the ion charge (represented by the black distribution, rounded to the nearest integer), ion mass (red), and ion energy (blue, truncated due to instrumentation constraints) values all affect the ion frequency. Broader distributions, such as ion energy (blue) in this scheme, affect the range of ion frequencies more than parameters that are narrowly distributed, such as mass (red). If any of the generated ion frequencies overlap (bottom plot, red X), they are discarded from the simulation

the average number of usable ions is divided by 0.37, corresponding to the maximum percentage of ion events that are usable when data from only single-ion trapping events are used [26, 44].

As the only simulated parameter that is completely determined by the data analysis method used, the characteristic FT peak width corresponding to the length of time domain segment used is a vital parameter in determining the maximum gain in CDMS acquisition rates. Narrower peak widths enable more unique ion frequencies to "fit" in a single trapping event without overlap within the frequency space established by the ion mass, charge, and energy distributions, resulting in faster overall ion acquisition. In Figure 3, the ideal relationship between FT length and peak base width for unapodized signal with a constant frequency is shown in red. Apodization of FT signals results in broader FT peaks regardless of the apodization function and is therefore undesirable in the context of multiple ion analysis in CDMS. For example, the commonly used Hanning apodization doubles the peak base width for a given FT length, as shown in gray in Figure 3. For model ion signals that do not vary in frequency over time, an FT of the entire trapping period results in the narrowest possible peaks, as peak widths vary as the inverse of FT length. However, multiple studies have shown that ion frequencies in CDMS do not remain constant for the duration of the trapping period [37–39, 43, 48, 49]. Collisions with background gas, neutral mass losses, and fragmentation all effect CDMS oscillation frequencies. If the ion signal frequency changes over the length of the FT, the peak width is broadened leading to signal amplitude that is distributed over multiple frequencies. This reduces the signal peak amplitude, resulting in a lower measured value of ion charge. As a result, short-time Fourier transforms (STFT) have been implemented to overcome this effect by transforming short segments in which the change in ion frequency is negligible [33, 38]. The amplitude data from each short segment is then averaged to calculate the charge, yielding the same precision typically obtained by using a single long FT on stationary signals.

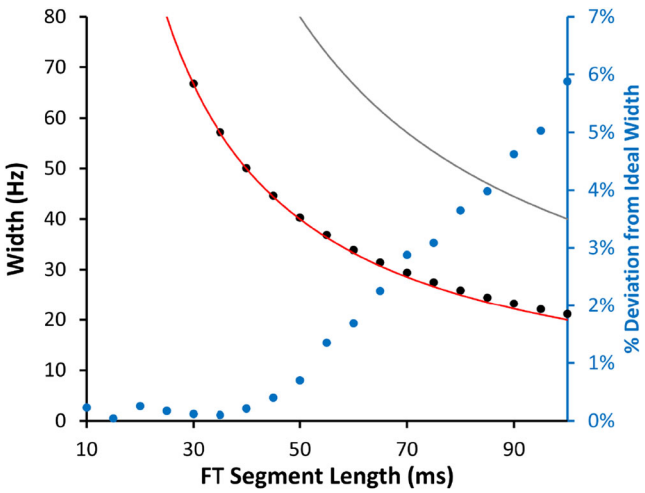

Figure 3. Effects of FT segment length and on ion frequency peak widths for experimentally measured RuBisCO ion signal. Ideal non-apodized (red) and Hanning-apodized (gray) peak widths are compared with the average measured width for 125, non-apodized experimental signals of RuBisCO ions (black) at different FT segment lengths. The RuBisCO data begin to slightly diverge from the ideal non-apodized signal around 40–50 ms owing to a gradual shift in frequency with time that occurs as a result of collisional energy loss and other factors. This divergence is more clearly observed in a plot of the % deviation from the ideal value, pictured here on a secondary axis (blue)

For multi-ion CDMS, the best choice of STFT segment length is the longest period that does not result in broadened peak widths and lowered amplitudes. This can be determined by analyzing the peak widths of the analyte of interest as a function of FT length. For example, Figure 3 shows the average base peak widths for the experimental data of 125 RuBisCO ions analyzed with different FT lengths incremented by 5 ms (black points). The RuBisCO peak width data begin to diverge from the ideal width (red) between ~40 and 50 ms, due to frequency shifting as a consequence of energy lost to collisions with background gas. This divergence is more apparent in the percentage of deviation from the ideal width (blue points, secondary axis in Figure 3). The FT length at which widths diverge from the ideal can vary significantly depending on instrumental conditions, such as the pressure in the trapping region and the trap design. Traps in which ion motion is more harmonic will lead to lower energy dependence on the oscillation frequency [42]. In this work, a virtual FT segment length of 50 ms corresponding to a 40 Hz base peak width was used in all simulations to make the results readily comparable to previous work. However, using this method to determine the ideal FT segment length in a multi-ion CDMS experiment is an important step in optimizing usable ion throughput.

Results and Discussion

Maximum Gains in Analysis Speed for Different Analytes

Using the simulation scheme described above, the optimum ion count and the gain in overall ion acquisition speed were determined for two analytes under different instrumental conditions. Analyte A has a nominal mass of 8 MDa and very broad mass and charge distributions, analogous to a sample of 8 MDa polyethylene glycol (PEG) studied in other CDMS work [29]. Analyte B has a nominal mass of 517 kDa and relatively narrow mass and charge distributions, analogous to the sample of RuBisCO in Figure 1a [43]. All of these analyte-specific parameters used in the simulations are provided in Table 1. Both analytes were simulated using three different sets of ion energy parameters, corresponding to different instrumental conditions. A narrow energy distribution (0.3% standard deviation), where frequency and m/z are closely coupled, corresponds to previous CDMS work where energy selective ion optics were employed [42]. An intermediate energy distribution (3% standard deviation), where there is significant

Table 1. Simulated Ion Parameters for Analytes A [43] and B [29]

Parameter	Analyte A	Analyte B
Mass (Da)	517,000	8,000,000
Mass standard deviation (Da)	1551	2,000,000
Charge (e)	51	800
Charge standard deviation (e)	1.8	100

decoupling, corresponds to recent multi-ion CDMS work [43]. Finally, a very broad energy distribution width (7.3% standard deviation) was simulated. This width was chosen such that ions within 1.5 standard deviations (~ 90% of all ions) would fall within the stability constraints imposed by current instrumentation [37]. The trap voltage is set to its current maximum of 500 V so that the absolute width of stable ion energies is as large as possible [39]. All parameters for these simulated energy distributions are provided in Table 2. Instrumentation capable of higher trap voltages and higher energy ion confinement could increase the absolute width of usable ion energies even further. Other decoupling gains might also be made via an improved trap design that stably confines ions with a wider energy distribution. However, these improvements were not studied here due to the trap design-specific parameters required to calculate ion energies and $C(E)$ in Eq. (1) [37–39].

Decoupling the frequency and m/z in CDMS greatly increases the number of ions which can be simultaneously analyzed, particularly for homogeneous samples. The gain in ion analysis speed as a function of the ion count is shown in Figure 4. For analyte A (circles), the gain in analysis speed is nearly linear with ion count for each different energy distribution. This is because the extremely broad mass and charge-state distributions of A result in a very broad range of possible frequencies regardless of the ion energy distribution and ion overlap events are rare even at higher ion counts. While greater decoupling does not yield large relative gains in ion throughput in this case, these results suggest that very large gains are possible for heterogeneous samples by measuring many ions using CDMS. Further simulations of A at ion counts up to 100 result in ion throughput gains of up to ~ 160×. This is lower than the ideal value of 270× because even for a very heterogeneous sample, the frequency space is still finite so the probability of overlap becomes more significant with a large number of trapped ions. In these cases, gains in usable signal can still be obtained by using the energy decoupling scheme. Ions produced from samples like A will be highly charged so it is possible that ion-ion interactions will ultimately limit the number of ions that can be simultaneously analyzed in an actual CDMS experiment. The extent to which ion-ion interactions are limiting can be determined from experimental measurements of ion mass as a function of the number of ions trapped [39] or potentially from ion trajectory simulations.

In the case of relatively homogeneous samples, such as analyte B (squares), ion frequency and m/z decoupling have a much more significant effect on the ion throughput gains, as shown in Figure 4. The three plots corresponding to the narrow (blue), intermediate (black), and broad (red) energy distributions of analyte B all have the same characteristic shape. The initial linear increase in gain is due to the low probability of ion overlap at low ion counts. The plots then level off as overlap events become more probable, eventually reaching a maximum. The maximum represents the ion count at which an ion added to the trapping event has equal probabilities of overlapping or not overlapping with another ion. After reaching the maximum, the slow decline in gain occurs as the high probability of ion overlap results in fewer usable ions. The maximum gain in analysis speed and corresponding ion count vary significantly depending on the extent of decoupling. Analyte B ions with a narrow distribution of ion energies (blue) reaches a maximum gain of ~ 19× at an ion count of ~ 20, whereas B ions with the broadest energy distribution (red) reach a maximum gain of ~ 48× at an ion count of ~ 45, meaning that greater extent of decoupling has the potential to more than double the overall analysis speed for analyte B ions using optimum ion currents. In both cases, the maximum gain in analysis speed is significantly higher than the ~ 10× improvement demonstrated in previous multi-ion CDMS work [43] because the average ion count/current was lower than the optimum value. To further corroborate this conclusion, the results from the intermediate energy distribution (black) match well with experimental results under closely comparable conditions. When an average of ~ 6 RuBisCO ions were trapped, there was a frequency overlap rate of ~ 15% [43]; for an ion count of 6 in this simulation, 1093 out of 6000 ions (18.2%) were discarded as a result of overlap. This close correlation between our simulations and previous experimental results suggests that these simulations serve as reasonably accurate predictors of CDMS data, strengthening our conclusions that further gains in CDMS ion analysis speed through ion multiplexing and decoupling frequency from m/z are possible. Another important conclusion from these data is that while the absolute gains in analysis speed depend on the ion count and analyte identity, it is always advantageous to maximize the extent of decoupling to obtain more usable ion signal. Ion-ion effects are not included in these simulations and these interactions may ultimately limit the extent of multiplexing that is experimentally achievable.

Table 2. Parameters for Simulated Ion Energy Distributions

Energy distribution	Mean energy per charge (eV/z)	Energy per charge standard deviation (eV/z)	Trapping voltage (V)	Stable trapping range (eV/z)
Narrow	230	0.7	330	195–245
Intermediate	230	7	330	195–245
Broad	342.5	25	500	305–380

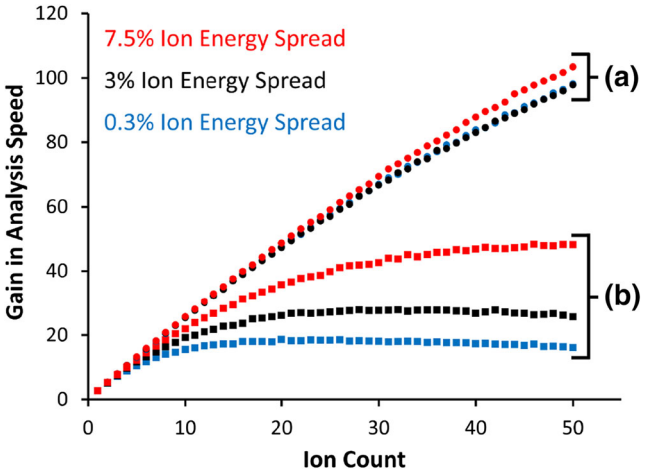

Figure 4. Simulated gains in analysis speed for analytes **(a)** and **(b)**. For analyte A, the ion energy distribution width makes only a minor difference in the observed gain. For analyte B, increasing the ion energy spread results in significantly higher gains in analysis speed

Improved Quantitation and Dynamic Range Via Decoupling

In addition to gains in analysis speed, decoupling ion frequency and *m/z* in CDMS can also yield greater dynamic range and provide more accurate quantitation in experiments where multiple ions are trapped. This is illustrated in Figure 5, where the simulated frequency histograms for 1000 trapping events for analyte B are shown at narrow, intermediate, and maximized ion energy distribution widths (rows) for ion counts of 1, 10, and 25 (columns). For an ion count of 1 (left column), the narrow ion energy distribution (top row) produces a resolved charge-state distribution in the frequency histogram where the abundance of each charge state is accurately reproduced. However, as the ion count increases to 10 (center column), the number of ions making up each peak in the charge-state distribution no longer accurately reflect the true values. Ions within the most abundant charge states are more likely to overlap in frequency and be discarded, resulting in a histogram skewed towards low abundance ions. This effect becomes very apparent at an ion count of 25 (right column). Resolution also decreases as a function of ion count. Outlier ions with frequencies that fall in between charge states are less likely to experience overlap and are retained disproportionally. For the intermediate ion energy distribution (middle row), the skew towards outliers is significantly decreased and is only visible as a small dip in the histogram for an ion count of 25. The charge-state resolution in the frequency histogram is lost, but because the *m/z* of each ion is obtained from both the frequency and ion energy measurements, the charge-state distribution in *m/z* space is resolved. For the broadest ion energy distribution (bottom row), the skew towards outliers is almost entirely mitigated at all ion counts. The irregular shape of the frequency distributions for the broadest energy distribution is due to a limited range of ion energies that can be trapped and a non-linear relationship between ion energy and frequency. The frequency is higher because the mean ion energy and corresponding trap voltage in the simulation are higher. While the charge-state distributions cannot be resolved in the frequency histogram for broader energy distributions, the *m/z* histograms generated from these frequency data still contain resolved charge-state distributions. Thus, no mass information is lost as a result of this frequency decoupling method as long as the energy and

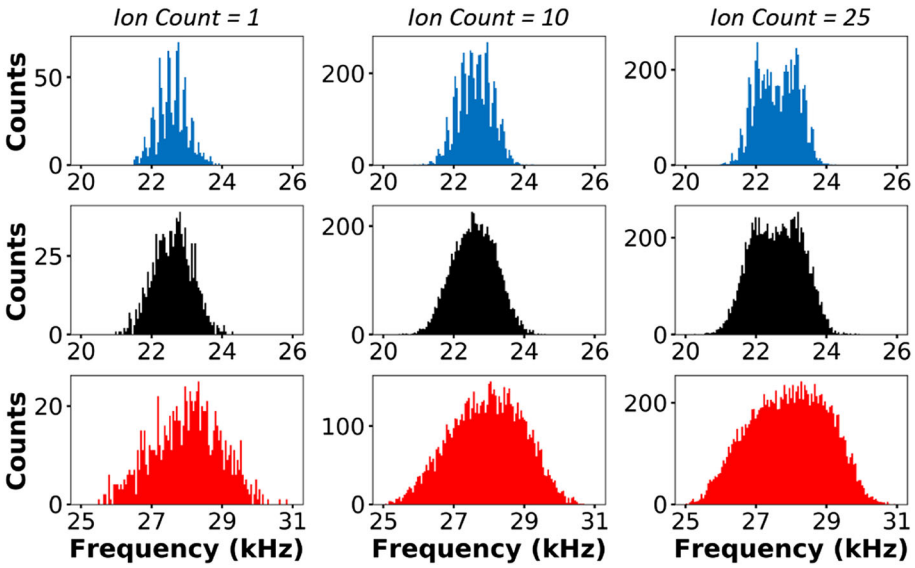

Figure 5. Simulated frequency histograms with different ion counts (1, 10, and 25) and different ion energy distribution widths (standard deviations of 0.3%, 3%, and 7.5%, rows, top to bottom). At low ion count, the narrowest energy distribution yields a charge state resolved, quantitative histogram. As ion count increases, quantitation is lost, as the most probable ions are suppressed by frequent overlap events. This quantitation error is mitigated in the lower histograms because overlap is less likely when the ion energy distributions are broad

charge of each ion is measured individually, as demonstrated elsewhere [37, 39, 43].

While the skewing effect observed in the narrow and intermediate energy distributions of Figure 5 does not affect the mass measurement of individual ions, it can affect the accuracy of quantitation and dynamic range of a sample containing two or more analytes. For example, if the abundance ratio of two analytes contained in a sample is 25:1, a trapping event with an ion count of 26 will contain, on average, 25 ions of the more abundant species and only one ion of the low abundance species. Using the narrow energy distribution described above, an ion count of 25 for the high abundance component results in ~6.8 usable ions after overlapping ions are discarded. If the low abundance ion occupies a different *m*/*z* and frequency space than that of the high abundance ion, it will very rarely experience overlap due to its low ion count. This results in an apparent abundance ratio of 6.8:1, nearly 4× lower than the true value. Decoupling ion *m*/*z* and frequency via a broader energy distribution can help mitigate this effect. For the same 25:1 true abundance ratio, the broadest energy distribution described above yields an apparent ratio of 14.7:1, 58.9% of the true value. In both cases, the high abundance component is under sampled because only multi-ion events with zero overlap will provide exact quantitation.

In multi-ion CDMS experiments, a more accurate measure of the true abundance ratios can be obtained by selecting trapping events that have the lowest number (ideally zero) of overlap events to use in the abundance calculation. Using lower than the optimum multiplexing ion current may also help to mitigate this effect in exchange for relatively small losses in analysis speed, i.e., using lower ion counts in the region where changes in the gain of analysis speed are minimal (Figure 4). Regardless of the methods used, abundances measured using a broad energy distribution will have significantly reduced quantitation error due to the significantly lower probability of overlap at all ion counts. This advantage, in addition to the larger gains in analysis speed, makes the maximum decoupling of ion frequency and *m*/*z* highly advantageous for multi-ion CDMS.

Conclusions

Simulations of ion signals for existing CDMS instrumentation demonstrate that the time necessary to acquire single-ion CDMS mass histograms can be greatly reduced by analyzing many simultaneously trapped ions. This gain in analysis speed can be increased further by decoupling ion *m*/*z* from the measured ion frequency. Decoupling is achieved by introducing ions with a broad range of energies into the CDMS ion trap. No mass information is lost as a result of decoupling because ion energies are measured dynamically for each individual ion. Compared to prior CDMS experiments where only trapping events containing a single ion were analyzed [26], these simulations show that up to a ~48× increase in analysis speed is achievable for homogeneous samples of large molecules such as large protein complexes, viruses, and other biological macromolecules that CDMS is well-suited to analyze. Using only trapping events containing a single ion, CDMS experiments using 100 ms trapping events and optimum ion currents require ~30–60 min to measure a usable mass histogram for a relatively homogeneous analyte [42, 44]. Using the methods described here, the acquisition time of a similar histogram can potentially be reduced to less than 1 min. For heterogeneous samples of large molecules such as polymers, analysis speed increases of up to ~160× are predicted, although actual experimental gains may be limited by ion-ion interactions inside of the trap.

CDMS has a nearly unlimited mass range, does not require homogeneous samples, and dynamic measurements that can also provide information about collisional cross sections [38, 39] and fragmentation pathways [37, 50] of individual ions. This makes CDMS an ideal choice for the native MS analysis of large, biologically relevant macromolecules and heterogeneous mixtures of large molecules that are too large or too heterogeneous to be analyzed with conventional mass spectrometers. Continued advances in CDMS technology have increased the sensitivity and accuracy of the method to the point where the intrinsic heterogeneity in the mass of large molecules of interest is nearly equal to or exceeds the experimental error in mass determination [26, 42, 43]. Similar to other single-ion measurements, such as those performed using FTICR [13] and Orbitrap [16] instruments, a principal limitation in CDMS has been the time required to acquire a statistically meaningful set of individual ion data. Using multi-ion CDMS, this throughput limitation has largely been surmounted and further gains in acquisition speed seem reasonably attainable with improvements in instrument design.

Acknowledgements

This material is based upon work supported by the National Science Foundation under CHE-1609866.

References

1. Susa, A.C., Xia, Z., Williams, E.R.: Native Mass Spectrometry from Common Buffers with Salts that Mimic the Extracellular Environment. Angew Chem Int Ed. **56**, 7912–7915 (2017)
2. Gavriilidou, A.F.M., Gülbakan, B., Zenobi, R.: Influence of Ammonium Acetate Concentration on Receptor–Ligand Binding Affinities Measured by Native Nano ESI-MS: A Systematic Study. Anal Chem. **87**, 10378–10384 (2015)
3. Loo, J.A.: Electrospray Ionization Mass Spectrometry: A Technology for Studying Noncovalent Macromolecular Complexes. Int J Mass Spectrom. **200**, 175–186 (2000)
4. Wysocki, V.H., Jones, C.M., Galhena, A.S., Blackwell, A.E.: Surface-Induced Dissociation shows Potential to be More Informative than Collision-Induced Dissociation for Structural Studies of Large Systems. J Am Soc Mass Spectrom. **19**, 903–913 (2008)
5. Benesch, J.L.P., Aquilina, J.A., Ruotolo, B.T., Sobott, F., Robinson, C.V.: Tandem Mass Spectrometry Reveals the Quaternary Organization of Macromolecular Assemblies. Chem Biol. **13**, 597–605 (2006)
6. Lössl, P., Snijder, J., Heck, A.J.R.: Boundaries of Mass Resolution in Native Mass Spectrometry. J Am Soc Mass Spectrom. **25**, 906–917 (2014)

7. O'Connor, P.B., McLafferty, F.W.: Oligomer Characterization of 4–23 kDa Polymers by Electrospray Fourier Transform Mass Spectrometry. J Am Chem Soc. **117**, 12826–12831 (1995)
8. Robb, D.B., Brown, J.M., Morris, M., Blades, M.W.: Method of Atmospheric Pressure Charge Stripping for Electrospray Ionization Mass Spectrometry and its Application for the Analysis of Large Poly(Ethylene Glycol)s. Anal Chem. **86**, 9644–9652 (2014)
9. McKay, A.R., Ruotolo, B.T., Ilag, L.L., Robinson, C.V.: Mass Measurements of Increased Accuracy Resolve Heterogeneous Populations of Intact Ribosomes. J Am Chem Soc. **128**, 11433–11442 (2006)
10. Morgner, N., Robinson, C.V.: Massign: An Assignment Strategy for Maximizing Information from the Mass Spectra of Heterogeneous Protein Assemblies. Anal Chem. **84**, 2939–2948 (2012)
11. Sader, J.E., Hanay, M.S., Neumann, A.P., Roukes, M.L.: Mass Spectrometry using Nanomechanical Systems: Beyond the Point-Mass Approximation. Nano Lett. **18**, 1608–1614 (2018)
12. Hanay, M.S., Kelber, S., Naik, A.K., Chi, D., Hentz, S., Bullard, E.C., Colinet, E., Duraffourg, L., Roukes, M.L.: Single-Protein Nanomechanical Mass Spectrometry in Real Time. Nat Nanotechnol. **7**, 602–608 (2012)
13. Smith, R.D., Cheng, X., Brace, J.E., Hofstadler, S.A., Anderson, G.A.: Trapping, Detection and Reaction of very Large Single Molecular Ions by Mass Spectrometry. Nature. **369**, 137–139 (1994)
14. Bruce, J.E., Cheng, X., Bakhtiar, R., Wu, Q., Hofstadler, S.A., Anderson, G.A., Smith, R.D.: Trapping, Detection, and Mass Measurement of Individual Ions in a Fourier Transform Ion Cyclotron Resonance Mass Spectrometer. J Am Chem Soc. **116**, 7839–7847 (1994)
15. Makarov, A., Denisov, E.: Dynamics of Ions of Intact Proteins in the Orbitrap Mass Analyzer. J Am Chem Soc. **20**, 1486–1495 (2009)
16. Kafader, J.O., Melani, R.D., Senko, M.W., Makarov, A.A., Kelleher, N.L., Compton, P.D.: Measurement of Individual Ions Sharply Increases the Resolution of Orbitrap Mass Spectra of Proteins. Anal Chem. **91**, 2776–2783 (2019)
17. Wuerker, R.F., Shelton, H., Langmuir, R.V.: Electrodynamic Containment of Charged Particles. J Appl Phys. **30**, 342–349 (1959)
18. Philip, M.A., Gelbard, F., Arnold, S.: An Absolute Method for Aerosol Particle Mass and Charge Measurement. J Colloid Interface Sci. **91**, 507–515 (1983)
19. Hars, G., Tass, Z.: Application of Quadrupole Ion Trap for the Accurate Mass Determination of Submicron Size Charged Particles. J Appl Phys. **77**, 4245–4250 (1995)
20. Schlemmer, S., Illemann, J., Wellert, S., Gerlich, D.: Nondestructive High-Resolution and Absolute Mass Determination of Single Charged Particles in a Three-Dimensional Quadrupole Trap. J Appl Phys. **90**, 5410–5418 (2001)
21. Howder, C.R., Bell, D.M., Anderson, S.L.: Optically Detected, Single Nanoparticle Mass Spectrometer with Pre-Filtered Electrospray Nanoparticle Source. Rev Sci Instrum. **85**, 014104 (2014)
22. Twerenbold, D.: Biopolymer Mass Spectrometer with Cryogenic Particle Detectors. Nucl Inst Methods Phys Res A. **370**, 253–255 (1996)
23. Sipe, D.M., Plath, L.D., Aksenov, A.A., Feldman, J.S., Bier, M.E.: Characterization of Mega-Dalton-Sized Nanoparticles by Superconducting Tunnel Junction Cryodetection Mass Spectrometry. ACS Nano. **12**, 2591–2602 (2018)
24. Barney, B.L., Pratt, S.N., Austin, D.E.: Survivability of Bare, Individual Bacillus Subtilis Spores to High-Velocity Surface Impact: Implications for Microbial Transfer through Space. Planet Space Sci. **125**, 20–26 (2016)
25. Benner, W.H.: A Gated Electrostatic Ion Trap to Repetitiously Measure the Charge and *M/Z* of Large Electrospray Ions. Anal Chem. **69**, 4162–4168 (1997)
26. Keifer, D.Z., Pierson, E.E., Jarrold, M.F.: Charge Detection Mass Spectrometry: Weighing Heavier Things. Analyst. **142**, 1654–1671 (2017)
27. Keifer, D.Z., Jarrold, M.F.: Single-Molecule Mass Spectrometry. Mass Spectrom Rev. **36**, 715–733 (2017)
28. Doussineau, T., Bao, C.Y., Antoine, R., Dugourd, P., Zhang, W., D'Agosto, F., Charleux, B.: Direct Molar Mass Determination of Self-Assembled Amphiphilic Block Copolymer Nanoobjects using Electrospray-Charge Detection Mass Spectrometry. ACS Macro Lett. **1**, 414–417 (2012)
29. Elliott, A.G., Merenbloom, S.I., Chakrabarty, S., Williams, E.R.: Single Particle Analyzer of Mass: A Charge Detection Mass Spectrometer with a Multi-Detector Electrostatic Ion Trap. Int J Mass Spectrom. **414**, 45–55 (2017)
30. Adamson, B.D., Miller, M.E.C., Continetti, R.E.: The Aerosol Impact Spectrometer: A Versatile Platform for Studying the Velocity Dependence of Nanoparticle-Surface Impact Phenomena. EPJ Tech Instrum. **4**(2), (2017)
31. Lutomski, C.A., Lyktey, N.A., Pierson, E.E., Zhao, Z., Zlotnick, A., Jarrold, M.F.: Multiple Pathways in Capsid Assembly. J Am Chem Soc. **140**, 5784–5790 (2018)
32. Lutomski, C.A., Gordon, S.M., Remaley, A.T., Jarrold, M.F.: Resolution of Lipoprotein Subclasses by Charge Detection Mass Spectrometry. Anal Chem. **90**, 6353–6356 (2018)
33. Pierson, E.E., Contino, N.C., Keifer, D.Z., Jarrold, M.F.: Charge Detection Mass Spectrometry for Single Ions with an Uncertainty in the Charge Measurement of 0.65 E. J Am Soc Mass Spectrom. **26**, 1213–1220 (2015)
34. Pierson, E.E., Keifer, D.Z., Asokan, A., Jarrold, M.F.: Resolving Adeno-Associated Viral Particle Diversity with Charge Detection Mass Spectrometry. Anal Chem. **88**, 6718–6725 (2016)
35. Keifer, D.Z., Pierson, E.E., Hogan, J.A., Bedwell, G.J., Prevelige, P.E., Jarrold, M.F.: Charge Detection Mass Spectrometry of Bacteriophage P22 Procapsid Distributions Above 20 MDa. Rapid Commun Mass Spectrom. **28**, 483–488 (2014)
36. Pierson, E.E., Keifer, D.Z., Contino, N.C., Jarrold, M.F.: Probing Higher Order Multimers of Pyruvate Kinase with Charge Detection Mass Spectrometry. Int J Mass Spectrom. **337**, 50–56 (2013)
37. Elliott, A.G., Harper, C.C., Lin, H., Williams, E.R.: Mass, Mobility and MS^N Measurements of Single Ions using Charge Detection Mass Spectrometry. Analyst. **142**, 2760–2769 (2017)
38. Elliott, A.G., Harper, C.C., Lin, H., Susa, A.C., Xia, Z., Williams, E.R.: Simultaneous Measurements of Mass and Collisional Cross-Section of Single Ions with Charge Detection Mass Spectrometry. Anal Chem. **89**, 7701–7708 (2017)
39. Harper, C.C., Elliott, A.G., Lin, H., Williams, E.R.: Determining Energies and Cross Sections of Individual Ions using Higher-Order Harmonics in Fourier Transform Charge Detection Mass Spectrometry (FT-CDMS). J Am Soc Mass Spectrom. **29**, 1861–1869 (2018)
40. Keifer, D.Z., Motwani, T., Teschke, C.M., Jarrold, M.F.: Acquiring Structural Information on Virus Particles with Charge Detection Mass Spectrometry. J Am Soc Mass Spectrom. **27**, 1028–1036 (2016)
41. Keifer, D.Z., Shinholt, D.L., Jarrold, M.F.: Charge Detection Mass Spectrometry with almost Perfect Charge Accuracy. Anal Chem. **87**, 10330–10337 (2015)
42. Hogan, J.A., Jarrold, M.F.: Optimized Electrostatic Linear Ion Trap for Charge Detection Mass Spectrometry. J Am Soc Mass Spectrom. **29**, 2086–2095 (2018)
43. Harper, C.C., Elliott, A.G., Oltrogge, L.M., Savage, D.F., Williams, E.R.: Multiplexed Charge Detection Mass Spectrometry for High-Throughput Single Ion Analysis of Large Molecules. Anal Chem. **91**, 7458–7465 (2019).
44. Draper, B.E., Jarrold, M.F.: Real-Time Analysis and Signal Optimization for Charge Detection Mass Spectrometry. J Am Soc Mass Spectrom. **30**, 898–904 (2019)
45. Marshall, A.G., Hendrickson, C.L., Jackson, G.S.: Fourier Transform Ion Cyclotron Resonance Mass Spectrometry: A Primer. Mass Spectrom Rev. **17**, 1–35 (1998)
46. Contino, N.C., Jarrold, M.F.: Charge Detection Mass Spectrometry for Single Ions with a Limit of Detection of 30 Charges. Int J Mass Spectrom. **345–347**, 153–159 (2013)
47. Ledford, E.B., Rempel, D.L., Gross, M.L.: Space Charge Effects in Fourier Transform Mass Spectrometry. II. Mass Calibration. Anal Chem. **56**, 2744–2748 (1984)
48. Keifer, D.Z., Alexander, A.W., Jarrold, M.F.: Spontaneous Mass and Charge Losses from Single Multi-Megadalton Ions Studied by Charge Detection Mass Spectrometry. J Am Soc Mass Spectrom. **28**, 498–506 (2017)
49. Elliott, A.G., Harper, C.C., Lin, H., Williams, E.R.: Effects of Individual Ion Energies on Charge Measurements in Fourier Transform Charge Detection Mass Spectrometry (FT-CDMS). J Am Soc Mass Spectrom. **30**, 946–955 (2018)
50. Halim, M.A., Clavier, C., Dagany, X., Kerleroux, M., Dugourd, P., Dunbar, R.C., Antoine, R.: Infrared Laser Dissociation of Single Megadalton Polymer Ions in a Gated Electrostatic Ion Trap: The Added Value of Statistical Analysis of Individual Events. Phys Chem Chem Phys. **20**, 11959–11966 (2018)